Strojniški vestnik - Journal of Mechanical Engineering 52(2006)12, 863-872
UDK - UDC 621.436:621.43.06
Izvirni znanstveni članek - Original scientific paper (1.01)

Raziskava učinkov različnih stopenj vračanja izpušnih plinov na temperaturo plamena in nastanek saj pri uporabi dizelskega goriva z različnimi T90 temperaturami destilacije

Experimental Study of the Effects of Different Exhaust Gas Recirculation Ratios on the Flame Temperature and Soot Formation when Using Diesel Fuels With Different T90 Distillation Temperatures

Danilo Nikolić[1] - Radoje Vujadinović[1] - Norimasa Iida[2]
([1]University of Montenegro, Podgorica, Montenegro; [2] KEIO University, Yokohama, Japan)

V študiji, opisani v tem prispevku, smo preizkušali krmiljenje dušikovega oksida (NOx) in nastanek saj. Kot razredčilo, pri simulaciji kroženja izpušnih plinov, smo uporabili ogljikov dioksid (CO_2) vsebnosti 4,3%, 9,5 in 14,3%, kar pomeni vsebnosti kisika (O_2) 20%, 19% in 18%. V nadaljevanju smo uporabili tri različna dizelska goriva z različnimi T90 temperaturami destilacije. Lastnosti goriva smo zavarovali pred vplivi vsebnosti aromatov, žvepla in cetanskega števila. Za simulacijo dizelskega zgorevanja smo uporabili hitrokompresijski motor z enim cilindrom. Postopek vžiga in zgorevanje pri vbrizgavanju dizelskega goriva smo opazovali s pomočjo hitrega neposrednega fotografiranja. Temperaturo plamena (kazalnik nastanka NO) in faktor KL (kazalnik vsebnosti saj v vbrizgu dizelskega goriva) smo analizirali z uporabo dvobarvne metode. Preizkus je pokazal, da se s povečanjem vsebnosti CO_2 v dovodu zmanjšata najvišja temperatura plamena in nastajanje saj. Prav tako so rezultati pokazali, da pri vsebnosti CO_2 = 4,3% v dovodu, T90 temperatura destilacije nima posebnega vpliva na najvišjo temperaturo plamena in nastanek saj.

(Ključne besede: gorivo dizelsko, plini izpušni, nastanek saj, temperatura destilacije)

In this paper the diesel in-cylinder control of nitrogen oxide (NOx) and soot formation was tested. Carbon dioxide (CO_2) was used as a diluent to simulate the exhaust-gas recirculation (EGR) process at ratios of 4.3%, 9.5% and 14.3%, thus making oxygen (O_2) concentrations of 20%, 19% and 18% respectively. In addition, three diesel fuels with different T90 distillation temperatures were used. The fuel parameters were isolated from the influence of the aromatics content, sulfur content, and cetane number. A single-cylinder rapid compression machine (RCM) was used to simulate the diesel-type combustion. The ignition and combustion processes of the diesel-fuel spray were observed using high-speed direct photography. The flame temperature (an indication of NO formation) and KL factor (an indication of the soot concentration inside the diesel-fuel spray) were analyzed using the two-color method. The study demonstrated that with an increase of the CO_2 concentration in the intake charge, the maximum flame temperature and the soot formation decrease. Also, when there was a CO_2=4.3% concentration in the intake charge, the results showed no significant influence of the diesel-fuel T90 distillation temperature on the maximum flame temperature and the soot formation.

(Keywords: diesel fuels, exhaust gas recirculation (EGR), distillation temperature, rapid compression machine)

0 INTRODUCTION

The environmental impact of motor vehicles is of great concern worldwide. In particular, the contribution to atmospheric pollution from motor vehicles points to the need to reduce vehicular emissions. Relative to the spark-ignited internal combustion engine, the diesel engine emits large quantities

of particulate matter (PM) and nitrogen oxide (NOx). It is difficult to reduce both of these pollutants at the same time because of their trade-off. Diesel emission-reduction strategies can be divided into two main types: in-cylinder control and after-treatment. In-cylinder control implies changes to the design of the engine and diesel-fuel reformulation, with the former providing more opportunities to reduce emissions [1].

Exhaust-gas recirculation (EGR) is an effective in-cylinder technique that reduces NOx because it lowers the maximum flame temperature. But the application of EGR can also adversely affect the quality of the lubricating oil, the engine durability and produce higher unburned hydrocarbon (HC) and PM exhaust emissions, resulting from the lower oxygen (O_2) concentration. The influence of EGR on exhaust emissions can be efficiently simulated by the addition of carbon dioxide (CO_2) to the intake charge. Ladommatos et al. [2] identified three major effects of introducing CO_2 into the intake charge of a diesel engine: the dilution effect, the chemical effect, and the thermal effect. The dilution effect, which represents the reduction in O_2 and nitrogen (N_2) fractions in the intake charge due to the replacement with CO_2, was shown to be the most significant, having an influence on both the combustion process and exhaust emissions. With the increase of CO_2 in the intake charge, the ignition delay periods increase ([3] to [7]), the NOx formation decreases ([4] to [7]), while soot formation in some cases increases ([8] and [5]) and in other cases decreases ([4] and [6]).

Many studies have been carried out to assess the effect of the fuel properties on diesel emissions. These studies showed that the fuel properties, such as the cetane number, the aromatic content and type, the distillation temperature, the density, and the viscosity, are the most influential on the combustion process and exhaust emissions. Many papers ([9] to [13]) have investigated the influence of the T90 distillation temperature of diesel fuels on exhaust emissions. Most of them reported an increase of NOx and PM emissions with the increase in the T90 distillation temperature.

The aim of this study was to show the combined effects of the EGR and T90 distillation temperatures of diesel fuel on the formation of NOx and soot inside the combustion chamber. A rapid compression machine (RCM) was used to simulate diesel combustion, having a single fuel-spray injection in the high-temperature and high-pressure atmosphere of the surrounding gas. The RCM is capable of a diesel-fuel spray-combustion investigation with minimized influences of some parameters specific to a high-speed diesel engine. The ignition and the combustion processes of diesel-fuel spray were observed using high-speed direct photography. The flame temperature (an indication of NO formation) and KL factor (an indication of soot formation) were analyzed with the two-color method. The two-color method is based on the continuous radiation of soot particles during the burning diesel-fuel spray.

1 TEST EQUIPMENT AND CONDITIONS

The RCM, Figure 1, used in this study for the simulation of the diesel-combustion process is a duplicated single-diesel-type compression cycle after the combustion process, which is carried out in the environment of a constant volume with high temperature and high pressure. The RCM is a pancake-type combustion chamber with a diameter of 145 mm and a thickness of 48 mm, as illustrated in Figure 2. The single fuel spray from one nozzle hole was injected straight down and did not collide with the walls of the combustion chamber. The piston stroke during compression is 692mm. The ratio and the time of compression are 15.5 and 200ms, respectively.

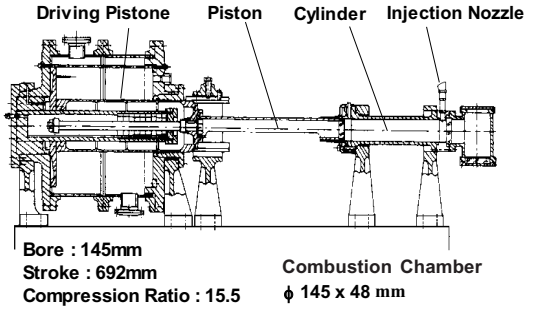

Fig. 1. *The Rapid Compression Machine*

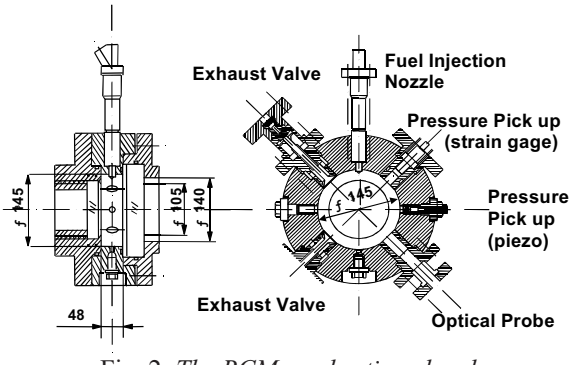

Fig. 2. *The RCM combustion chamber*

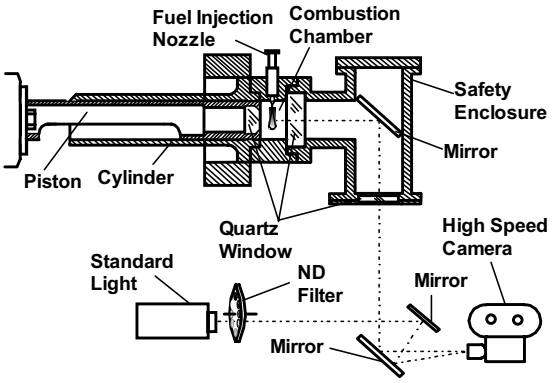

Fig. 3. *Optical arrangement*

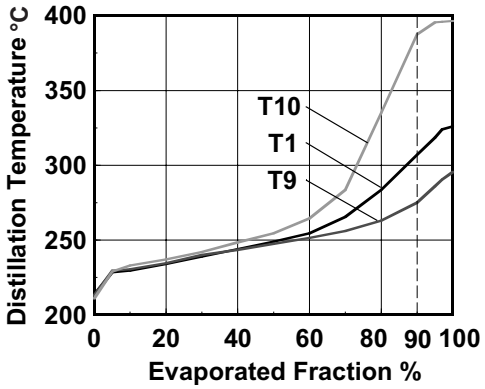

Fig. 4. *Distillation curves of the test fuels*

The in-cylinder pressure inside the RCM combustion chamber was measured with a piezo-electric sensor.

Observations and optical measurements were performed via the quartz windows installed on both the piston and the cylinder head. The image of the flame shape passed through the quartz window was reflected from two plane mirrors (one in the safety box and the other outside) and was caught by the high-speed camera. The speed of the high-speed camera is 5000 flashes per second (FPS) (Model: NAC 16 HD; Shutter constant: 5). The film used was Kodak VISION 500T 7279 (16 mm). Figure 3 shows the optical arrangement of the high-speed photography. The image of a halogen lamp, with a known luminous temperature, was also recorded on each frame as a standard light source for the two-color method analysis. This lamp was positioned at the optical distance from the camera that was equal to the fuel-spray flame.

This study involved high-speed direct photography of the luminous flames, a combustion analysis from pressure diagrams, and flame-temperature and KL-factor analyses by the two-color method applied to the color image of the luminous flames.

CO_2 was used as a diluent to simulate the EGR process at the ratios of 4.3%, 9.5% and 14.3%, thus making O_2 concentrations of 20%, 19% and 18%, respectively. Table 1 shows the composition and the state of the intake charge (gas). Table 2 shows the experimental conditions.

In the experiment, three JCAP (Japanese Clean Air Project) fuels were used, T1, T9, and T10, each with a different T90 distillation temperature. The influence of the T90 was isolated from the influences of the aromatics content (0%), the sulfur content (0%), and the cetane number. Some types of n-paraffins and i-paraffins were mixed to keep the cetane number constant. Table 3 shows the main properties of the test fuels, while Figure 4 shows their distillation curves.

Figure 5 shows the chromatogram data analyzed by Miwa [14]. The fuels with a higher T90 contain heavier elements.

Table 1. *Composition and state of the intake charge*

	O_2 vol %	CO_2 vol %	N_2 vol %	Ar vol %	T_{in} K	T_0 K	P_{in} MPa	P_0 MPa
Air + CO_2	21	0	78	1	353	905±5	0.1	3.0±0.1
	20	4.3	74.2	0.95	353	895±5	0.1	3.0±0.1
	19	9.5	70.5	0.91	353	885±5	0.1	3.0±0.1
	18	14.3	66.8	0.86	353	875±5	0.1	3.0±0.1

Table 2. *Experimental conditions*

Max. Inj. Pressure	P_{inj}	70 MPa
Nozzle Hole Diameters	d	0.18 mm
Fuel-Injection Period	T_{inj}	4.0±0.1 MPa
Injection Equipment		JERK type Fuel Pump
Injection-valve Opening pressure	P_{op}	23 MPa

Table 3. *Properties of the test fuels*

Fuel properties	unit	**T1**	**T9**	**T10**
Density @15°C	g/cm^3	0.7880	0.7852	0.7916
Viscosity@30°C	mm^2/s	3.630	3.322	4.946
Cetane Number		48.8	48.6	48.5
Distillation				
IBP	°C	213.5	213.0	211.0
10%	°C	229.5	230.5	233.0
50%	°C	249.0	247.5	254.5
90%	°C	307.0	275.0	387.5
EP	°C	326.0	295.5	396.5
Sulfur	mass %	0	0	0
Mean Molecular Weight		206	202	219
Lower Calorific Value	J/g	43910	43920	43970
C/H Ratio	(atom/ atom)	0.476	0.479	0.479
n-Paraffin	% (v/v)	36	35	24
i-Paraffin	% (v/v)	57	59	70
Naphthene	% (v/v)	7	6	6
Total-Aromatics	% (v/v)	0	0	0

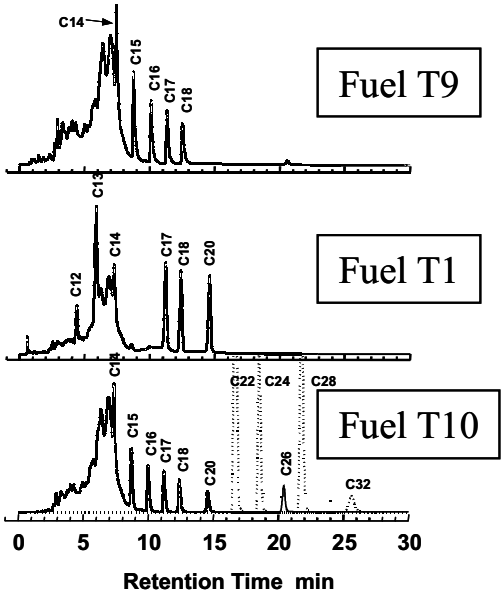

Fig. 5. *Chromatograms of the test fuels*

Figure 6 shows the time histories of the in-cylinder pressure and temperature when only air was compressed. The fuel injection was set to begin at 60 ms after the RCM drive piston reached its top position.

After the in-cylinder pressure reaches its maximum at the top dead center (TDC) and constant-volume conditions begin, the in-cylinder pressure gradually declines due to heat losses and gas leakages. T_o and p_o are the in-cylinder temperature and pressure at the time of the fuel injection.

1.1 Definition of the ignition delay time and the characteristic combustion times

Figure 7 shows a typical example of the in-cylinder pressure rise at the time of the fuel injection and during combustion, and the fuel-injection pressure and the needle-lift histories. When the fuel was injected, mixture cooling occurred and the in-cylinder pressure decreased more rapidly. The time from the start of the fuel injection to the start of the heat release was defined as the ignition delay time

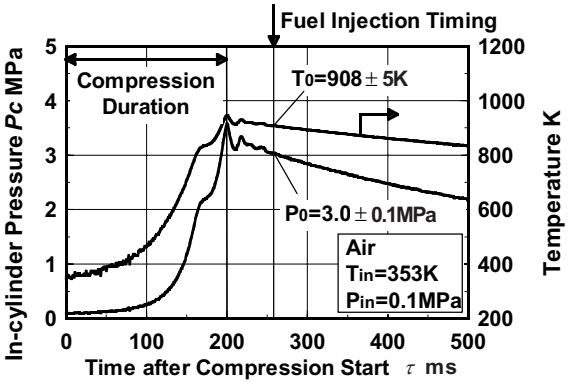

Fig. 6. *Typical in-cylinder pressure and temperature histories for the RCM*

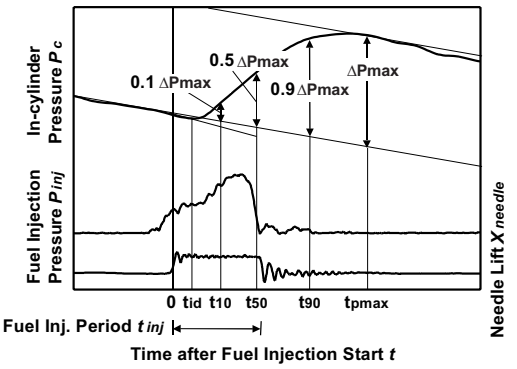

Fig. 7. *Model of in-cylinder pressure, fuel-injection pressure and needle lift*

t_{id}, while the time from the start of the fuel injection to the peak of in-cylinder pressure was defined as t_{Pmax}.

The in-cylinder pressure increase was defined as ΔP_{max}, and the times to reach 10%, 50% and 90% of the peak pressures (ΔP_{max}) were defined as t_{10}, t_{50} and t_{90}, respectively. Because the equivalence ratio was rather small, the specific heat during combustion was assumed to be nearly constant, and thus the burnt-fuel fraction and the pressure increase were considered almost proportional. Therefore, t_{10}, t_{50} and t_{90} could be considered as 10%, 50% and 90% of the burned-fuel timings. The time from the start of the fuel injection to the first appearance of the luminous flame was defined as t_{fa}, and the time of the luminous flame's disappearance was defined as t_{fd}.

2 RESULTS AND DISCUSSION

Figure 8 shows examples of two-dimensional direct photograph images of the T10 fuel-spray combustion for all the test conditions. With the increase of the CO_2 concentration in the intake charge, the luminous flame area and the intensity of the flame decrease. A similar trend appears for the T1 and T9 fuels.

Figure 9 shows pressure diagrams for all the test conditions and the test fuels. During compression and at the time of the fuel injection, the pressure of the intake charge (gas mixture) decreases as the CO_2 concentration increases, maintaining lower pressures during the whole combustion period. This pressure decrease with the increase of the CO_2 concentration in the intake charge is the reason for

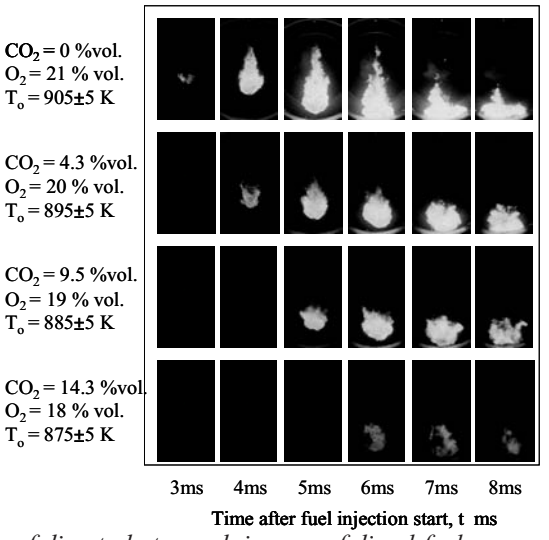

Fig. 8. *Examples of direct photograph images of diesel-fuel spray combustion (fuel T10)*

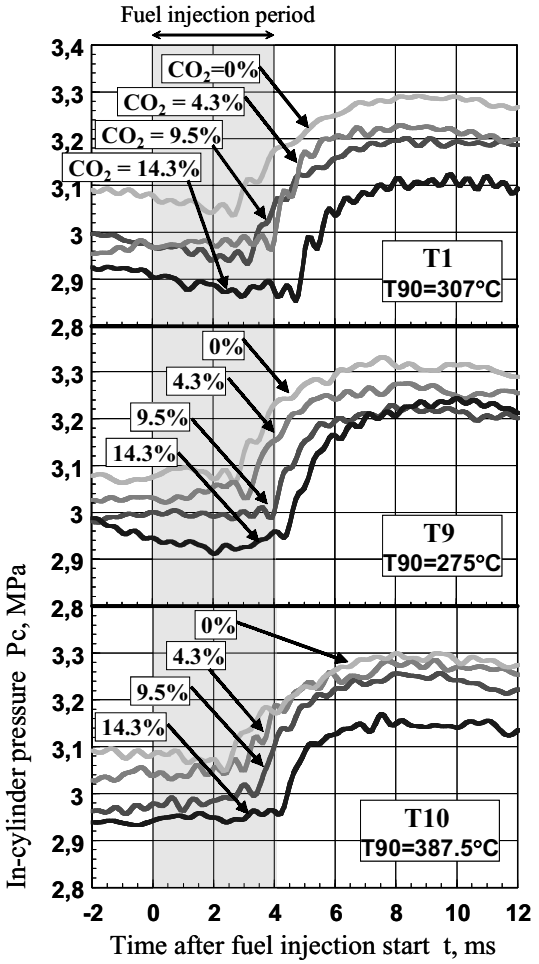

Fig. 9. *In-cylinder pressure histories*

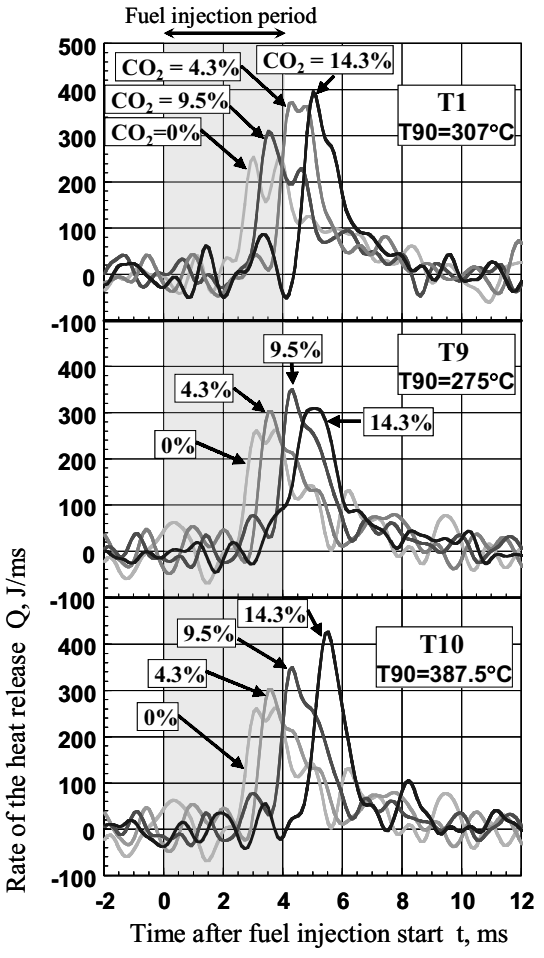

Fig. 10. *Rate of the heat-release-time histories*

the changed composition of the combustion air and could be associated with the increase of the specific heat of such a mixture.

Figure 10 shows the rate-of-heat-release (RHR) diagrams for all the test conditions and the test fuels. With the increase of the CO_2 concentration in the intake charge the high peaks of the RHR increase and are delayed. This is caused by the increased ignition delay, which means that at the time of the ignition there is more fuel available in the cylinder, well mixed, and with a faster burning rate after the ignition.

Figure 11 shows the relationships between the ignition delays, the luminous-flame appearance times, the luminous-flame periods and the combustion periods with characteristic times. The ignition-delay periods are longer with the increase of CO_2 concentrations. This is caused by the decrease of O_2 concentrations in the intake charge as well as the decrease of the intake gas temperature and pressure at the moment of the diesel-fuel injection. This fact makes the periods of fuel/gas-mixture preparation longer. The luminous-flame appearance times (the start of soot radiation) follow the same trend as the ignition delay periods. The luminous-flame periods and combustion periods decrease with the increase of the CO_2 concentration in the intake charge. This could be due to a prolonged ignition delay, the decrease of the O_2 concentrations from 21% to 18%, the lower in-cylinder temperatures and pressures, which all contribute to incomplete combustion.

Figure 12 shows an example of two-dimensional images of the flame temperature and the KL value distribution inside the diesel-fuel spray flame determined by the two-color method. In the case of CO_2=14.3%, due to the low luminosity of the flame, the two-color method was not applicable.

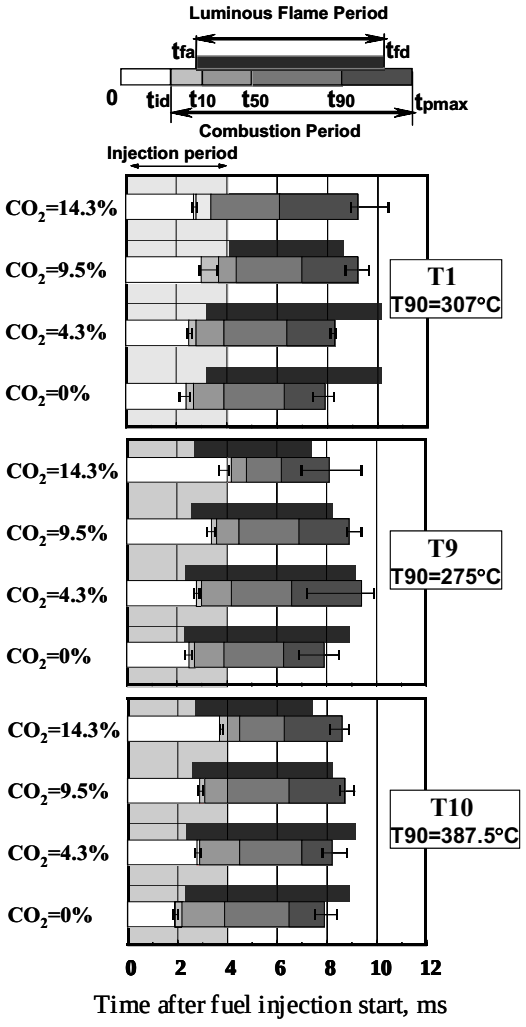

Fig. 11. *Ignition delays, characteristic combustion periods and luminous-flame periods*

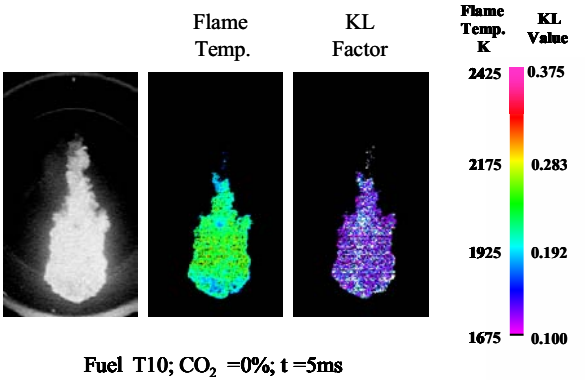

Fig. 12. *Examples of direct photograph images of luminous fuel spray flame, temperature and KL factor distribution in the fuel spray flame*

Figure 13 (at the end of the paper) shows the time histories of the luminous-flame area and the flame-temperature distribution inside the fuel-spray flames. The flame temperatures obtained from the image analysis using the two-color method were hierarchies at 100K intervals, starting from 1750K. There are decreases in the luminous-flame areas and in the high-temperature areas with the increase of the CO_2 concentrations in the intake charge.

Figure 13 also shows the area-averaged flame temperature, which is defined by the ratio of $\Sigma A_i T_i / \Sigma A_i$, in which T_i is the median value of each hierarchy, A_i is the area having temperature T_i, and ΣA_i is the total flame area. The maximum values of this temperature decrease with the increase of the CO_2 concentration in the intake charge. This decrease is more obvious for CO_2 concentrations of 4.3% and higher. This decrease is a consequence of the O_2 concentration decrease in the combustion chamber and the increase of the inert gases, the decrease of the intake-charge temperatures and the pressures at the time of the fuel injection as well as during the whole combustion period. Regarding the T90 distillation temperature of the diesel fuel, there is a decrease in the maximum area-averaged flame temperature as well as the duration of high temperatures with a decrease of the T90 distillation temperature in the cases of CO_2=0% and CO_2=9.5%. In the case of CO_2=4.3% there is no significant difference in the maximum area-averaged flame temperatures as well as in the duration of the high temperatures.

Figure 14 shows the time history of the area-integrated KL value. The KL value is a multiple of the absorption coefficient K, which is nearly proportional to the soot-particle number density in the flame (Beers law) and the optical path length L in the soot region. The KL value is an index of the total number of soot particles along the optical path. The area-integrated KL value $\Sigma A_i(KL)_i$ was defined as the product of the median value of each hierarchy $(KL)_i$ and its area, A_i.

With the increase of the CO_2 concentration in the intake charge, soot starts forming later due to increased ignition delays. The maximum area-integrated KL values decrease with the increase of the CO_2 concentration. It was expected that there would be more soot formed with the increase of CO_2 concentration due to a lower O_2 concentration. Lower values of the area-integrated KL value with the increase of CO_2 concentration could be the result of a more homogeneous mixture at the time of the ignition due to more time being available for mixture

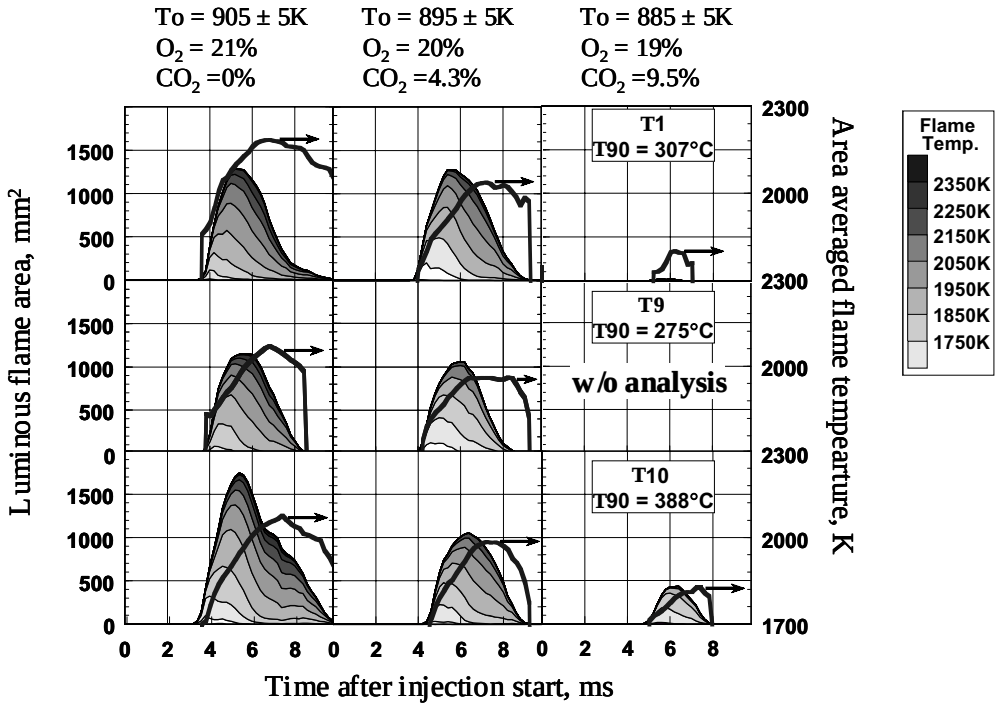

Fig. 13. *Time histories of temperature distribution inside diesel fuel spray flame and of area averaged flame temperature*

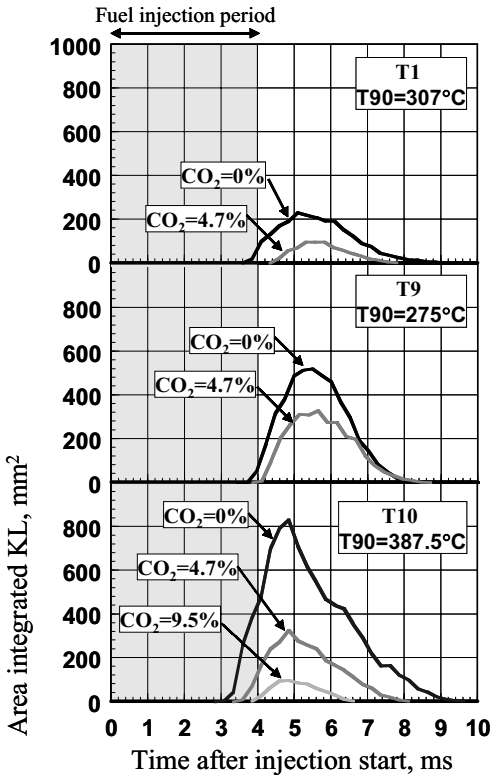

Fig. 14. *Time history of the area-integrated KL values*

preparation, due to lower temperatures inside combustion chamber at the time of the ignition, as well during the whole combustion period, and due to the fact that there is still enough air in such a big combustion chamber, which supports soot oxidation. Iida SAE950213 and Mitchell SAE932798 published similar results. The period of the KL existence decreases with the increase of CO_2 concentration in the intake charge, except for the fuel T9 with the lowest T90 distillation temperature. The KL existence period could be related to the soot exhaust emissions from a real diesel engine. By lowering the intake-gas temperature it is possible to use higher EGR rates, which will significantly lower NOx and, at the same time, not influence significantly the soot-formation and soot-extinction periods. Regarding the effect of the fuel on soot formation and emission, for cases of CO_2=0% and 9.5%, the soot-extinction periods decrease with the decrease of the T90 distillation temperature. For the case of CO_2=4.3%, there is a slight influence of the T90 distillation temperature on the soot-formation and soot-existence periods. This means that by using this CO_2 concentration there is a possibility to use heavier fuels for the same soot exhaust emission.

3 CONCLUSION

In this study exhaust gas recirculation (EGR) was simulated by the introduction of carbon dioxide (CO_2) into the intake air for four different concentrations, 0%, 4.3%, 9.5%, and 14.3%, using three diesel fuels with different T90 distillation temperatures of 275ºC, 307ºC, and 387.5ºC, in order to determine the influence on the nitrogen oxide (NOx) and soot formation inside the combustion chamber of a rapid compression machine (RCM).

The main conclusions from this study are as follows:

- Maximum flame temperature (NOx formation) decreases with CO_2 concentration increase in the intake charge.
- Soot formation and existence periods decrease with CO_2 concentration increase in the intake charge.
- The fuel with the lowest T90 distillation temperature, T9, showed a good soot-NOx trade-off in the case without any CO_2 addition to the intake charge.
- The fuel with the highest T90 distillation temperature, T10, showed a good soot-NOx trade-off in the case of CO_2=4.3% in the intake charge.

4 REFERENCES

[1] K.Mitchell (2000) Effects of fuel properties and source on emission from five different heavy duty Diesel engines, *SAE Paper No. 2000-01-2890*.

[2] N.Ladommatos, S.M.Abdelhalim, H.Zhao and Z.Hu (1996) The dilution, chemical and thermal effects of exhaust gas recirculation on Diesel engine emission – Part1: Effects of reducing inlet charge Oxygen, *SAE Paper No. 961165*.

[3] D. Nikolic, K. Wakimoto, S. Takahashi and N. Iida (2001) Effect of nozzle diameter and EGR ratio on the flame temperature and soot formation for various fuels, *SAE Paper No. 2001-01-1939*.

[4] D.L.Mitchell, J.A.Pinson and T.A.Litzinger (1993) The effects of simulated EGR via intake air dilution on combustion in an optically accessible DI Diesel engine, *SAE Paper No. 932798*.

[5] N.Ladommatos, S.M.Abdelhalim, H.Zhao and Z.Hu (1996) The dilution, chemical and thermal effects of exhaust gas recirculation on Diesel engine emission – Part2: Effects of Carbon Dioxide, *SAE Paper No. 961167*.

[6] N.Iida (1996) Surrounding gas effects on soot formation and extinction – Observations of Diesel spray combustion using a rapid compression machine, *SAE Paper No. 960603.*

[7] S.Ropke, G.W.Schweimer and T.S.Strauss. NOx formation in Diesel engines for various fuels and intake gases, *SAE Paper No. 950213.*

[8] A.M.Kreso, J.H.Johnson, L.D.Gratz, S.T.Bagley and D.G.Leddy (1998) A study of the effects of exhaust gas recirculation on heavy duty Diesel engine emissions, *SAE Paper No. 981422.*

[9] K.Nakakita, S.Takasu, H.Ban, T.Ogawa, H.Naruse, Y.Tsukasaki and L.I.Yeh (1998) Effect of hydrocarbon molecular on Diesel exhaust emissions – Part 1: Comparison of combustion and exhaust emission characteristics among representative Diesel fuels, *SAE Paper No. 982494.*

[10] N.Miyamoto, H. Ogawa, M.Shibuya, K.Arai, and O.Esmilaire (1994) Influence of the Hydrocarbon fuels on Diesel exhaust emissions, *SAE Paper No. 940676.*

[11] M.Tamanouchi, H.Morihisa, S.Yamada, J.Iida, T.Sasaki and H.Sue (1997) Effects of fuel properties on exhaust emissions for Diesel engines with and without oxidation catalyst and high pressure injection, S*AE Paper No. 970758.*

[12] W.S.Neill, W. L.Chippior, O.L.Gulder, J.Cooley, E.K.Richardson, K.Mitchell and C.Fairbridge (2000) Influence of fuel aromatics type on the particulate matter and NOx emissions of a H.D. Diesel engine, S*AE Paper No. 2000-01-1856.*

[13] K.Tsurutani, Y.Takei, Y. Fujimoto, J. Matsudaira and M. Kumamoto (1995). The effects of fuel properties and oxygenates on Diesel exhaust emissions, *SAE Paper No. 952349.*

[14] Consignment research report concerning influence of Diesel engine technology and fuel technology on exhaust emission, *Petroleum Energy Center* PEC-1999JC-25 (1999).

Authors' Addresses: Prof. Dr. Danilo Nikolić
Doc. Dr. Radoje Vujadinović
University of Montenegro
Cetinjski put bb
81000 Podgorica, Montenegro
dannikol@cg.yu

Prof. Dr. Norimasa Iida
KEIO University
3-14-1 Hiyoshi, Kohoku-ku
Yokohama 223-8522, Japan
iida@sd.keio.ac.jp

Prejeto: 13.3.2006
Received:
Sprejeto: 25.10.2006
Accepted:
Odprto za diskusijo: 1 leto
Open for discussion: 1 year